Cardiomyocyte and vascular smooth muscle independent 11-hydroxysteroid dehydrogenase 1 amplifies infarct expansion, hypertrophy and the development of heart failure following myocardial infarction in male mice

Cardiomyocyte and vascular smooth muscle independent 11β-hydroxysteroid dehydrogenase 1 amplifies infarct expansion, hypertrophy and the development of heart failure following myocardial infarction in male mice

Christopher I White[1], Maurits A Jansen[1,2], Kieran McGregor[1], Katie J Mylonas[1], Rachel V Richardson[1], Adrian Thomson[2], Carmel M Moran[1,2], Jonathan R Seckl [1], Brian R Walker [1], Karen E Chapman[1] & Gillian A Gray[1]*

[1]BHF/University Centre for Cardiovascular Science, University of Edinburgh, Queens Medical Research Institute, 47 Little France Cres, Edinburgh EH16 4TJ, Scotland, UK.; [2]Edinburgh Preclinical Imaging, University of Edinburgh, College of Medicine & Veterinary Medicine, 47 Little France Cres, Edinburgh EH16 4TJ, Scotland, UK.

Global deficiency of 11β-hydroxysteroid dehydrogenase 1 (11β-HSD1), an enzyme that regenerates glucocorticoids within cells, promotes angiogenesis and reduces acute infarct expansion following myocardial infarction (MI) suggesting that 11β-HSD1 activity has an adverse influence on wound healing in the heart after MI. The present study investigated whether 11β-HSD1 deficiency could prevent the development of heart failure following MI, and examined whether 11β-HSD1 deficiency in cardiomyocytes and vascular smooth muscle cells confers this protection. Male mice with global deficiency in 11β-HSD1, or with *Hsd11b1* disruption in cardiac and vascular smooth muscle (via *SM22α-Cre* recombinase) underwent coronary artery ligation for induction of MI. Acute injury was equivalent in all groups. However, by 8 weeks after induction of MI, relative to C57Bl/6 wild type, globally 11β-HSD1 deficient mice had reduced infarct size (34.7±2.1%LV vs 44.0±3.3%LV, P=0.02), improved function (ejection fraction 33.5±2.5% vs 24.7±2.5%, P=0.03) and reduced ventricular dilation (LVEDV 0.17±0.01ml vs 0.21±0.01ml, P=0.01). This was accompanied by a reduction in hypertrophy, pulmonary edema and in the expression of genes encoding atrial natriuretic peptide and β-myosin heavy chain. None of these outcomes, nor promotion of peri-infarct angiogenesis during infarct repair, were recapitulated when 11β-HSD1 deficiency was restricted to cardiac and vascular smooth muscle. 11β-HSD1 expressed in cells other than cardiomyocytes or vascular smooth muscle limits angiogenesis and promotes infarct expansion with adverse ventricular remodeling after MI. Early pharmacological inhibition of 11β-HSD1 may offer a new therapeutic approach to prevent heart failure associated with ischemic heart disease.

Interventions to restore perfusion following myocardial infarction (MI) have significantly enhanced acute survival (1). However many patients survive with injury to their myocardium that is replaced during wound healing by noncontractile scar tissue. In the longer term structural, functional and metabolic remodeling of the remaining ventricle to compensate for contractile deficiency and alteration in wall stress promotes progression to heart failure (2). Retention of functional cardiomyocytes is critical in limiting subsequent adverse ventricular remodeling. In

ISSN Print 0013-7227 ISSN Online 1945-7170
Printed in USA

Received July 21, 2015. Accepted October 8, 2015.

Abbreviations:

experimental models cardiomyocyte loss can be reduced by intervention at the time of reperfusion, but successful translation of these interventions to the clinic has been limited (3, 4). Cardiomyocyte death also occurs in the peri-infarct area during infarct healing and scar formation, leading to infarct expansion. Promotion of angiogenesis during this phase can limit infarct expansion and subsequent adverse remodeling (5–9).

Glucocorticoids (physiological cortisol and corticosterone, as well as synthetic forms) are known to suppress angiogenesis (10). Plasma levels of cortisol increase in the hours after MI following activation of the hypothalamic-pituitary-adrenal axis and may protect cardiomyocytes from acute ischemic injury (11–13), but as circulating levels are reduced within days of MI, they are unlikely to impact on the later angiogenesis that is associated with infarct healing. However, active glucocorticoids can also be regenerated locally from circulating inert 11-keto metabolites by the enzyme, 11β-hydroxysteroid dehydrogenase type 1 (11β-HSD1), that is expressed in many cells, including in cardiomyocytes, fibroblasts, and smooth muscle cells in the heart (14). Genetic disruption of *Hsd11b1*, the gene encoding 11β-HSD1 does not change initial ischemic injury in the murine heart following experimental MI, but leads to enhancement of peri-infarct vessel density (8, 10). Importantly, vessels formed during infarct healing mature to maintain blood flow to the peri-infarct area in 11β-HSD1 deficient mice and increased vessel density is associated with shorter and thicker infarcts and with retention of cardiac function (8). Pharmacological inhibitors of 11β-HSD1 have reached phase 2 clinical development for use in diabetes and cognitive dysfunction and have potential as a new therapeutic approach for promotion of angiogenesis, including post-MI (15, 16). However, whether 11β-HSD1 deficiency can prevent maladaptive ventricular remodeling and progression to heart failure following MI has not been examined.

11β-HSD1 activity is not detectable in endothelial cells, but the enzyme is present in the vessel wall where expression and activity is associated with smooth muscle cells (17, 18). Whether glucocorticoids regenerated by 11β-HSD1 in vascular smooth muscle cells act as an endogenous brake upon angiogenesis in the healing infarct, or indeed upon any aspect of ventricular remodeling after MI, is unknown. A recent study has shown that myocardial expression of 11β-HSD1 is increased in an MI-independent model of pathological hypertrophy and that ventricular remodeling can be reversed by pharmacological inhibition of 11β-HSD1 without any change in vessel density (19). This suggests that 11β-HSD1 has effects in the heart over and above those involving angiogenesis, potentially via 11β-HSD1 expressed in cardiomyocytes.

The present study tested the hypothesis that long term maladaptive structural and functional myocardial remodelling and the development of heart failure following MI are attenuated by 11β-HSD1 deficiency. To establish the contribution of 11β-HSD1 specifically in vascular smooth muscle cells and cardiomyocytes to the beneficial outcome following MI seen in mice lacking the enzyme globally, targeted deletion of 11β-HSD1 in these cell types was investigated.

Materials and Methods

Experimental Animals. All experiments involving animals were approved by the University of Edinburgh Animal Welfare and Ethical Review Body and by the UK Home Office. Experiments used adult male (10–14 weeks of age) mice with global deficiency on a C57Bl/6 genetic background (*Hsd11b1*$^{-/-}$) (8, 20), with C57Bl/6 controls, or mice in which deletion was targeted to vascular smooth muscle and cardiomyocytes (21, 22). These *Hsd11b1*$^{fl/fl}$*Sm22α-Cre*$^{+}$ (*Hsd11b1*$^{CVCre+}$) were generated by crossing *Sm22α-Cre* mice with *Hsd11b1*$^{fl/fl}$ mice, homozygous for a "floxed" allele of *Hsd11b1* (generated by Artemis Pharmaceuticals, Cologne, Germany, directly onto a C57BL/6J background). LoxP sites were placed flanking exon 3 of the mouse *Hsd11b1* gene, excision of which results in a "null allele" by "out of frame splicing" from exon 2 to exon. Controls were *Hsd11b1*$^{fl/fl}$ *(Cre-)* littermates (*Hsd11b1*$^{CVCre-}$). Following *Cre* genotyping, appropriate targeting was confirmed by determination of *Hsd11b1* RNA and 11β-HSD1 protein content in myocardium, aorta, liver and skeletal muscle.

Induction of MI. Myocardial infarction (MI) was induced by coronary artery ligation (CAL, as previously described (8, 23)) in *Hsd11b1*$^{-/-}$ mice, in age matched C57Bl/6 mice (WT), in *Hsd11b1*$^{CVCre+}$ and in *Hsd11b1*$^{CVCre-}$ mice. Briefly, following injection of analgesic (buprenorphine, 0.05 mg/kg, s.c.) and intubation for mechanical ventilation (120 strokes/min, 200μl stroke volume, HSE-Harvard MiniVent), the chest was opened at the fourth intercostal space and the pericardium was removed to allow ligation of the left anterior descending coronary artery (LAD) (6–0 Prolene suture, Ethicon). Succesful ligation was confirmed by blanching of the left ventricle (LV), and the chest was closed using a 5–0 Mersilk suture (Ethicon), ensuring that no air remained in the chest cavity. The skin was closed using 9 mm stainless steel autoclips (Harvard Apparatus). Following surgery 1.5ml sterile saline (0.9%, s.c.) was administered to aid recovery. 24h after induction of MI, a blood sample (45μl) was collected from the tail vein into a tube containing sodium citrate buffer for assay of troponin I by ELISA (Life Diagnostics High Sensitivity Mouse Cardiac Troponin-I ELISA Kit) to assess the extent of injury (24).

Structural & Functional Characterization. 8 weeks after coronary artery ligation surgery, cardiac structure, function and infarct size was measured using magnetic resonance imaging (MRI), as previously described (25). Temperature was maintained at 37°C, respiration rate at 50–60 breaths per minute and

heart rate at 500–550 bpm during imaging in isoflurane (1.3–1.8%) anesthetized mice. Animals were placed in a supine position inside a 7T MRI scanner (Agilent Technologies) with a 39 mm quadrature radiofrequency coil. Short axis cardiac images were acquired using an ECG-triggered and respiratory gated gradient echo 'cine' sequence (TR/TE = 7.3/2.7ms with a flip angle of 15°) with gradient and RF spoiling. Nine consecutive 1 mm thick slices from 12–13 time frames were acquired, which encompassed the entire heart from base to apex. The field of view was 30 mm with a 192 × 192 matrix and 4 averages were used. ImageJ software (National Institutes of Health) was used to assess left ventricular (LV) end diastolic volume, LV end systolic volume, and ejection fraction. Infarct size was measured by segmenting each short axis image into 20 sections. Any section which was thinned and akinetic or dyskinetic over the cardiac cycle was designated as infarcted tissue. Gray scale contrast also allowed visual confirmation of infarcted tissue. Infarct length was quantified by adding together the endo and epicardial circumference of infarcted tissue and dividing this by the sum of the total endo and epicardial circumferences.

After MRI mice were killed by cervical dislocation and the lungs collected and weighed to assess pulmonary edema. Hearts were weighed and either frozen at −80°C for subsequent RNA extraction and analysis; or processed and embedded in paraffin wax for histological and immunohistochemical analysis.

In a separate study, *Hsd11b1*$^{CVCre+}$ and *Hsd11b1*$^{CVCre-}$ mice underwent CAL for induction of MI as above, or sham operation. Structure and function was investigated by high-resolution ultrasound (Vevo 770 High Resolution Ultrasound Scanner (Visualsonics) 7 days after surgery. Briefly, long axis views of the heart in ECG-Gated Kilohertz Visualization (EKV) mode and M-mode were acquired in isoflurane (2%) anesthetized mice placed on a heated table to maintain body temperature at 37°C, heart rate was maintained in the range of 500–550 bpm. Ventricular area at end systole (LV end systolic area, LVESA) and at end diastole (LV end diastolic area, LVEDA) were collected from EKV traces using Vevo Image Analysis Software (Visualsonics) and this permitted calculation of EF (EF). Fractional shortening (FS) was calculated from M-mode. In this study hearts were perfusion fixed in situ and prepared for histological assessment of infarct area, vessel density and macrophage content.

Molecular Analysis. RNA was extracted from homogenized tissue using a Trizol Plus RNA Purification Kit (Invitrogen) according to the manufacturers instructions. After confirmation of RNA concentration and the A_{260}/A_{280} ratio (Nanodrop 1000 Version 3.3, Thermo Scientific), each sample was DNase I treated to remove genomic DNA. RNA was reverse transcribed (High Capacity cDNA Reverse Transcription Kit, Applied Biosystems) and cDNA synthesis was performed in a thermal cycler using the following conditions; 25°C for 10 minutes, 48°C for 40 minutes, 95°C for 5 minutes, then cooled to 4°C. *Hsd11b1* expression was assessed for each sample in triplicate using a Taqman Gene Expression Assay (Mm00476182_m1). For cardiac genes qRT-PCR was performed to assess mRNA levels of atrial natriuretic peptide (ANP, *Nppa*), Collagen1α2 (*Col1a2*), Collagen 3α1 (*Col3a1*), transforming growth factor β (TGFβ, *Tgfb1*), α-myosin heavy chain (α–MHC, *Myh6*), and β- myosin heavy chain (β-MHC, *Myh7*) using a Lightcycler 480 (Roche) and the Taqman Fast Advanced template or the Roche Fam Hydrolysis (Roche) template as appropriate. The internal control for all qRT-PCR experiments was β-actin (*Actb*), which was similar in all groups. Primers (Table S1) were designed in house and prepared by Invitrogen. A standard curve was prepared by pooling 2 μl from each cDNA sample. and making serial dilutions in RNase-free water.

Western Blotting. 11β-HSD1 protein content was assessed by Western blot as previously described (26), in the heart, liver, aorta and skeletal muscle to confirm appropriate deletion in *Hsd11b1*$^{CVCre+}$ mice. Briefly 50 mg of tissue was homogenized in 300μl lysis buffer (RIPA buffer (Sigma), protease & phosphatase inhibitor cocktails (Sigma) then centrifuged at 12 000 G for 15 minutes at 4°C. Proteins were separated by SDS-PAGE then transferred (Trans-Blot Semi Dry Transfer Cell, Bio-Rad) to a nitrocellulose membrane. After blocking (milk powder in TBS buffer with Tween 20) the membrane was incubated overnight at 4°C with primary 11β-HSD1 antibody (1/10000 in 5% BSA, generated in house in sheep (26)). The membrane was washed before application of horse radish peroxidase (HRP) conjugated donkey-antisheep secondary antibody (1/5000, Abcam, ab97125) then washed again and exposed to antimouse β-actin (1/10000, Cell Signaling Technologies) as a loading control, to HRP conjugated rabbit antimouse secondary antibody (Abcam, ab6728) then developed (ECL Prime Western Blotting Detection Reagent (GE Healthcare) and exposed to X-ray film for detection. 11β-HSD1 protein levels was calculated by normalizing the density of this band to that of β-actin protein.

Histological and Immunohistochemical Analysis. Infarct area and thickness were assessed in Masson's Trichrome stained paraffin sections. The infarcted area was selected manually and expressed as a percentage of the total area of the LV (Image Pro 6.2 and a Stereologer Analyzer 6 (MediaCybernetics)). Infarct thickness was determined by averaging scar thickness from five equally-spaced points along the length of the infarct. For macrophages, slides were incubated overnight with biotinylated rat antimouse Mac 2 (1/6000, Cedarlane), or for alternatively activated macrophages with rabbit antimouse Ym1 (1/500, Stem Cell Technologies) followed by a biotinylated goat antirabbit (Vector). Color was developed with a few drops of diaminobenzidine (DAB, Vector) according to the manufacturers instructions. A color threshold was set manually so as to only select positive brown staining for Mac2 and the area of this positive staining within the infarct was calculated automatically. Total macrophage infiltration was then expressed as the percentage area of positive brown DAB staining within the infarct. Peri-infarct angiogenesis was assessed in tissue sections by detection of immunoreactive CD31 (rabbit antimouse CD31 (1/50, Abcam,) in PBS) with a biotinylated goat antirabbit (Vector) secondary antibody. DAB solution was added to each section for visualization. Angiogenesis was assessed in 20 randomly assigned fields of view around the infarct border. The number of $CD31^+$ vessels were measured and categorised according to size; capillaries (<4 μm diameter), small arterioles (4 – 200 μm diameter) and large arterioles (>200 μm diameter).

Cardiomyocyte cross-sectional area was assessed in isolectin B4 (Alexa Fluor conjugated isolectin B4 (1/100, Thermo Fisher) and wheat germ agglutinin (wheat germ agglutinin-rhodamine (1/75, Vector) stained paraffin sections as previously described (27). Five randomly selected regions of interest were visualized in the LV free wall. Adobe Photoshop CS5 Extended (Adobe) was

used to calculate cross-sectional area in cardiomyocytes which appeared to be cut in the short axis as judged by (a) a nucleus in the middle of the cell and, (b) surrounded by capillaries which were also cut in the short axis.

Statistical analysis. Prism 6f for Mac OS X (GraphPad Software Inc) was used for 2 way ANOVA (7 day *Hsd11b1*$^{CVCre+}$ and *Hsd11b1*$^{CVCre-}$, sham and MI) or two-tailed unpaired Student's *t* tests (comparisons of *Hsd11b1*$^{-/-}$ and WT, or *Hsd11b1*$^{CVCre+}$ and *Hsd11b1*$^{CVCre-}$) All values are expressed as mean ± SEM, statistical significance was accepted at $P < .05$.

Results

Global but not cardiomyocyte and vascular smooth muscle cell disruption of Hsd11b1 prevents infarct thinning and expansion during the development of heart failure

Hsd11b1 mRNA and 11β-HSD1 protein levels were both significantly reduced in the myocardium and aorta, but not in liver or skeletal muscle, of *Hsd11b1*$^{CVCre+}$ mice relative to their littermate controls (*Hsd11b1*$^{CVCre-}$), consistent with selective disruption of gene expression in cardiomyocytes and vascular smooth muscle directed by *SM22-α-Cre* (Figure 1) (21). Blood pressure, contractile function and heart weight:body weight ratio were not significantly different to wild type mice (Supplemental Figure 1). Troponin I in plasma collected from the tail vein 24h after coronary artery ligation, a measure of ischemic injury, increased to over 40 ng/ml in all groups (Supplemental Figure 2), confirming that the extent of the initiating myocardial injury is not influenced by 11β-HSD1 deficiency (8). In contrast, when injury was assessed at 8 weeks after MI (Figure 2), either in vivo by MRI or in histological sections, infarct area was significantly less ($P < .05$) and average thickness was significantly greater ($P < .005$) in mice with global 11β-HSD1 deficiency compared to their WT controls. This attenuation of infarct expansion was not seen in *Hsd11b1*$^{CVCre+}$ relative to their *Hsd11b1*$^{CVCre-}$ littermate controls (Figure 2c).

Ventricular dilation is reduced and function improved in mice with global, but not cardiomyocyte and vascular smooth muscle cell, depletion of Hsd11b1

Analysis of structural and functional remodeling by MRI 8 weeks after induction of MI revealed a significant reduction in LV end-diastolic and end-systolic volumes in mice with global, but not tissue-specific, depletion of 11β-HSD1 (Figure 3a, $P < .05$). Ejection fraction was increased by 41 ± 9% in *Hsd11b1*$^{-/-}$ mice (Figure 3b, $P < .05$), consistent with greater retention of contractile function in this group only. Lungs collected from *Hsd11b1*$^{-/-}$ mice 8 weeks after induction of MI were also significantly lighter (Figure 3c, $P < .05$) than WT mice or mice with tissue-specific deletion, suggesting that *Hsd11b1*$^{-/-}$ mice have reduced tendency to develop pulmonary edema.

Global but not cardiomyocyte and vascular smooth muscle cell depletion of Hsd11b1$^{-/-}$ reduces cardiac hypertrophy and expression of fetal genes

MRI analysis conducted at 8 weeks after induction of MI revealed a reduction in myocardial mass in *Hsd11b1*$^{-/-}$ (120 ± 7.3 mg) compared to WT mice (160 ± 5.7 mg, $P < .01$) and this was confirmed by postmortem gravimetric analysis (Figure 4a, $P < .001$). Reduced hypertrophic remodeling in hearts from *Hsd11b1*$^{-/-}$ mice was evidenced by a significant decrease in cardiomyocyte cross sectional area (Figure 4b, $P < .05$) and in the expression of the fetal cardiomyocyte markers α-MHC (relative to β-MHC, $P < .05$) and ANP ($P < .01$, Figure 4c), compared to their WT controls. Expression of the profibrotic genes *TGFB1*, and the *Col1a2* and *Col3a1* genes encoding the major collagens, was unaffected by global or cardiovascular specific deficiency of 11β-HSD1 (Figure 5).

Peri-infarct angiogenesis and infarct expansion at 7 days after induction of MI are not influenced by cardiomyocyte and vascular smooth muscle selective depletion of Hsd11b1

As long term outcomes following MI were not improved when *Hsd11b1* disruption was restricted to cardiomyocytes and vascular smooth muscle, a further study was conducted to investigate early wound healing and infarct expansion in these mice. By 7 days after induction of MI, during infarct repair, high resolution ultrasound showed that the extent of LV dilation and loss of function was similarly impaired in all mice relative to sham-operated mice (Figure 6a). Cardiomyocyte and vascular smooth muscle restricted deletion of *Hsd11b1* also failed to influence infarct size (Figure 6b) or the extent of peri-infarct angiogenesis during infarct healing (Figure 6c). Macrophage recruitment was increased post-MI relative to sham operation (Figure 6d), but neither recruitment nor polarization of macrophages towards a YM-1 positive 'M2' macrophage phenotype was influenced in hearts from *Hsd11b1*$^{CVCre+}$ compared to *Hsd11b1*$^{CVCre-}$ mice (Figure 6d).

Discussion

In this study we present three important findings: (1) that 11βHSD1 amplifies infarct expansion and progression to

heart failure after MI, supporting the use of pharmacological inhibitors of 11βHSD1 to prevent the development of heart failure in this setting; (2) that disruption of the *Hsd11b1* gene in cardiac muscle does not prevent the expression of fetal genes or hypertrophic remodeling after MI suggesting that 11βHSD1 in cardiomyocytes does not play a direct role in regulating this process; (3) that the promotion of peri-infarct angiogenesis associated with prevention of early infarct expansion in mice with global 11βHSD1 deficiency (8) does not involve 11βHSD1 in smooth muscle cells of the vessel wall.

Following MI, ventricular remodeling and heart failure develop in response to loss of contractile myocardial tissue that is not replaced after injury. The extent of this early injury is a key determinant of long-term outcome (28). In the present study, initial myocardial ischemic injury, as assessed by plasma levels of cardiac troponin I, was not influenced by 11β-HSD1 deficiency, confirming our previous observations where infarct injury was assessed directly early after MI (8). Glucocorticoids can protect the heart from ischemic injury, and systemic glucocorticoid, increased as a result of HPA activation in response to MI,

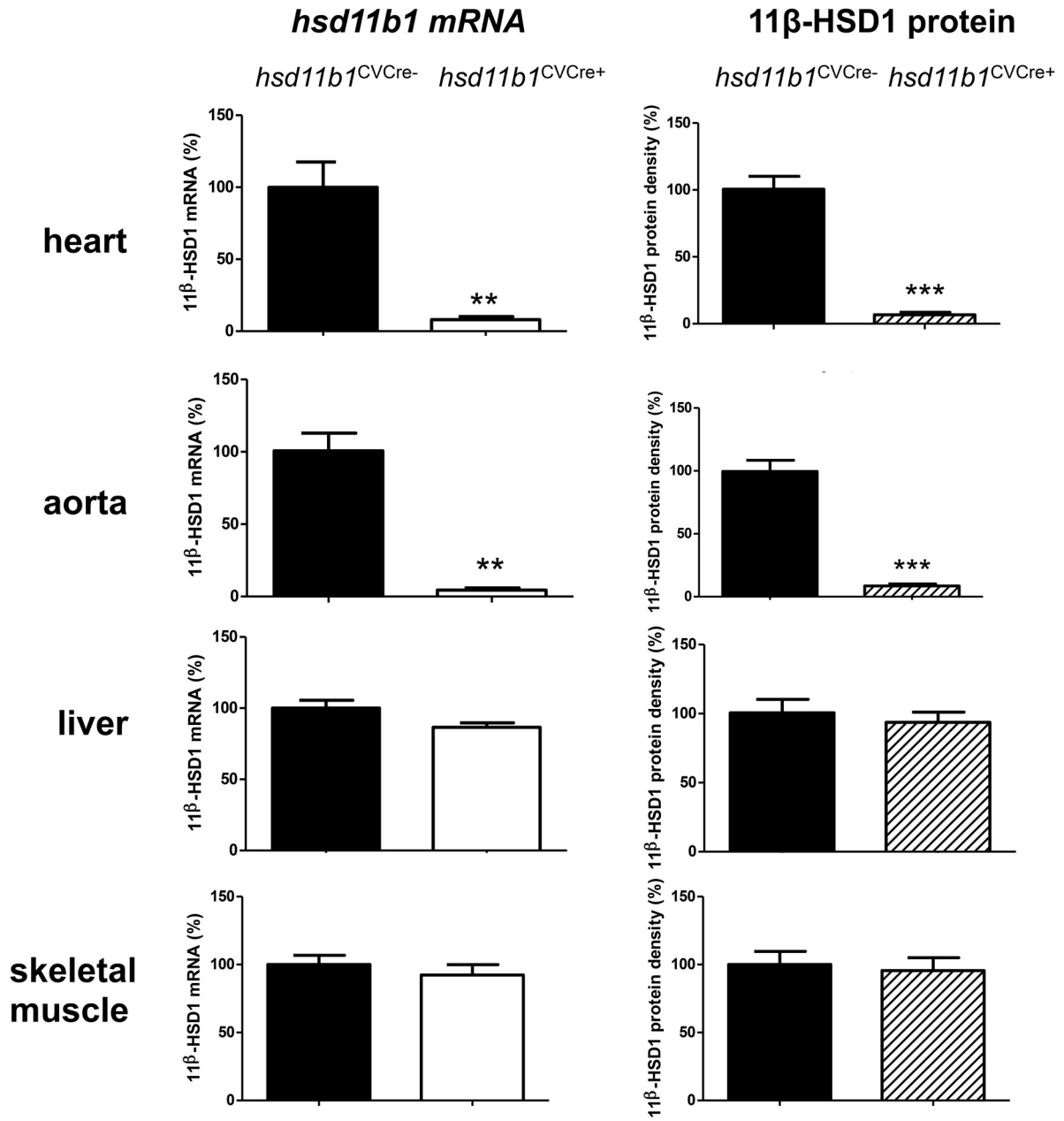

Figure 1. Confirmation of cardiovascular specific 11β-HSD1 deletion. *Hsd11b1* mRNA and 11β-HSD1 protein were assessed by rt-PCR (normalized to β-actin housekeeping gene) and Western blotting (normalized to β-actin loading control) respectively in heart, aorta, liver and skeletal muscle from *Hsd11b1*$^{fl/fl}$*Sm22α-Cre*$^{+}$ (*Hsd11b1*$^{CVCre+}$) and control *Hsd11b1*$^{fl/fl}$*Sm22α-Cre*$^{-}$ (*Hsd11b1*$^{CVCre-}$) mice. Expression in *hsd11b1*$^{CVCre+}$ is expressed relative to maximum achieved in tissue from *Hsd11b1*$^{CVCre-}$ *** $P < .001$, ** = $P < .01$ vs parallel control; n = 4/group.

is dominant in the first 24h after MI. We have already shown that this early peak in plasma glucocorticoid concentration after MI is not altered in 11β-HSD1 deficient mice, therefore it is not surprising that early injury is also unaffected in these mice (8). However by 8 weeks after induction of injury the infarct had expanded and thinned to a lesser degree in mice with global deficiency of 11β-HSD1, and this was associated with less ventricular dilation, a key prognostic indicator of outcome in human heart failure (2, 29). Decreased dilation in the present study was accompanied by diminished expression of ANP, consistent with lowered wall stress (30), as well as reduction of ventricular dysfunction and pulmonary edema, together indicating prevention of progression to heart failure. This outcome is consistent with a detrimental influence of 11β-HSD1 on wound healing and remodeling that occur in response to injury.

Replacement of damaged myocardium by noncontractile scar tissue induces cardiomyocytes in the noninfarcted ventricle to undergo hypertrophic remodelling to maintain cardiac output, resulting in an increase in myocardial mass. Here, heart mass, assessed either in vivo by MRI, or ex vivo gravimetrically, was reduced in mice with global deficiency in 11β-HSD1. As well as increased cross-sectional area, cardiomyocytes undergoing pathological hypertrophy show re-expression of fetal genes, including those encoding ANP and β myosin heavy chain (βMHC). Increased expression of βMHC relative to the adult αMHC isoform is associated with loss of cardiomyocyte contractility in murine models (31). In the present study it is clear that global deficiency in 11β-HSD1 suppresses hypertrophic remodeling and reduces re-expression of fetal genes consistent with retention of function and reduction of wall stress. Recent data have linked a common variation in the *Hsd11b1* gene to LV mass in man (32). Reversal of pathological hypertrophy by pharmacological inhibition of 11β-HSD1 in an MI-independent murine model also supports a specific role for 11β-HSD1 in the regulation of cardiomyocyte hypertrophy (19). However, neither modification of fetal genes, nor changes in myocyte cross sectional area were observed when *Hsd11b1* deletion was limited to cardiomyocytes and vascular smooth muscle. This is consistent with a mechanism that is dependent on prohypertrophic signaling from other cells in the heart that express 11β-HSD1. Indeed, residual expression of *Hsd11b1*, evident in RNA and protein analysis of hearts from *Hsd11b1Cre*$^{+ve}$ mice, supports sites of expression in the heart over and above cardiomyocytes and vascular smooth muscle. Transcriptomic analysis has revealed that *Hsdl11b1* is enriched 6-fold in cardiac fibro-

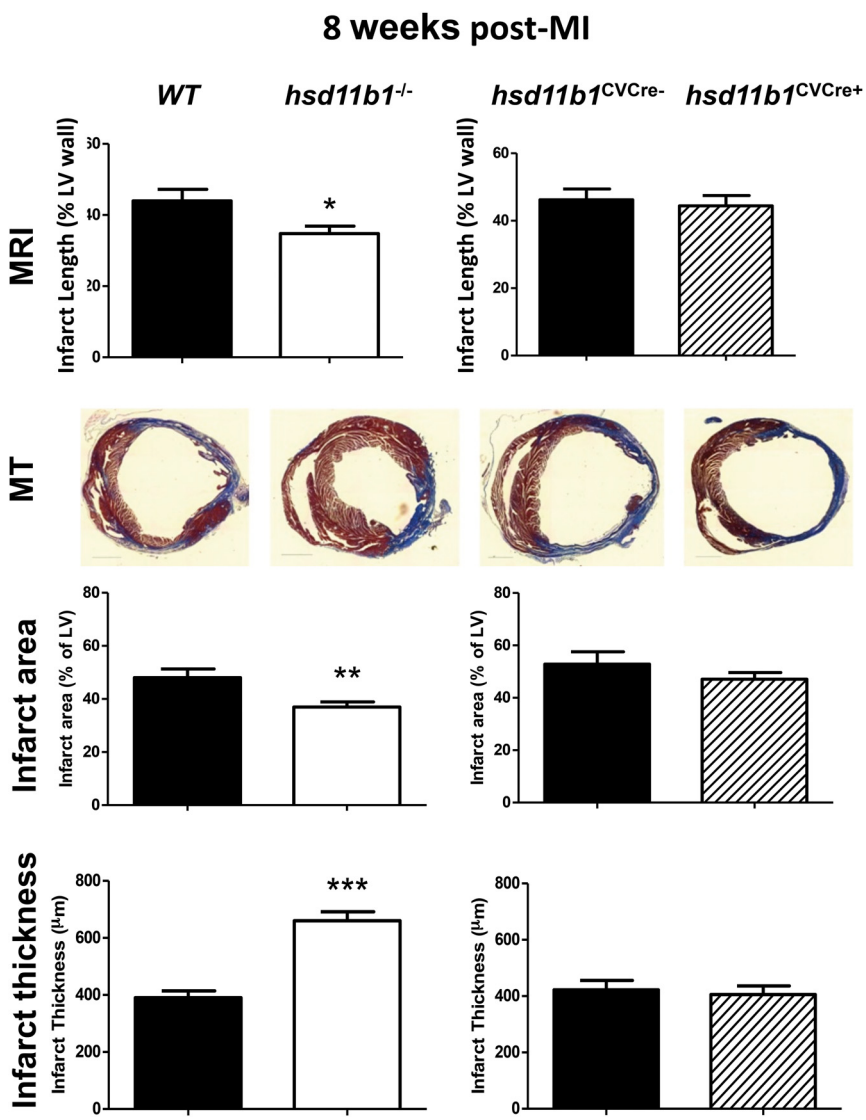

Figure 2. Global, but not cardiovascular specific, 11β-HSD1 deficiency reduces infarct expansion post-MI. Infarct injury was compared in wild type (WT) and global 11β-HSD1 deficient mice (*Hsd11b1*$^{-/-}$), and in mice with cardiomyocyte and vascular smooth muscle specific deletion (*Hsd11b1*$^{CVCre+}$) and respective control (*Hsd11b1*$^{CVCre-}$) at 8 weeks after induction of MI by (top panel) MRI and by (lower panels) histology (Masson's trichrome, MT) to determine infarct area and infarct thickness. Paired groups were compared by Student's *t* test * $P < .05$, ** $P < .01$, *** $P < .005$; n = 6–8/group.

blasts relative to fibroblasts from other sources (33). Fibroblasts release a number of immunomodulatory and hypertrophy regulating factors and could be a key site for local regulation of cardiomyocyte growth during remodeling (34, 35). 11β-HSD1 has previously been shown to regulate the release of inflammatory mediators in synovial fibroblasts (36, 37), and this mechanism merits further investigation in the heart. Resident or recruited myeloid cells also express *Hsd11b1* and can regulate cardiomyocyte hypertrophy (38, 39). Alternatively, if infarct size is the primary driver for adaptive hypertrophy following MI (28), then reduction of infarct expansion in mice with global 11β-HSD1 deficiency may be sufficient to diminish changes in cardiomyocyte gene expression and size. It is feasible that loss of 11β-HSD1 in other organs eg, the kidney have indirect effects on hemodynamic stress during the development of heart failure.

We have previously demonstrated that peri-infarct angiogenesis during infarct healing is enhanced in globally 11β-HSD1 deficient mice (8, 10) and that this is associated with development of shorter and thicker infarcts (8). *Hsd11b1* is expressed in the smooth muscle, but not the

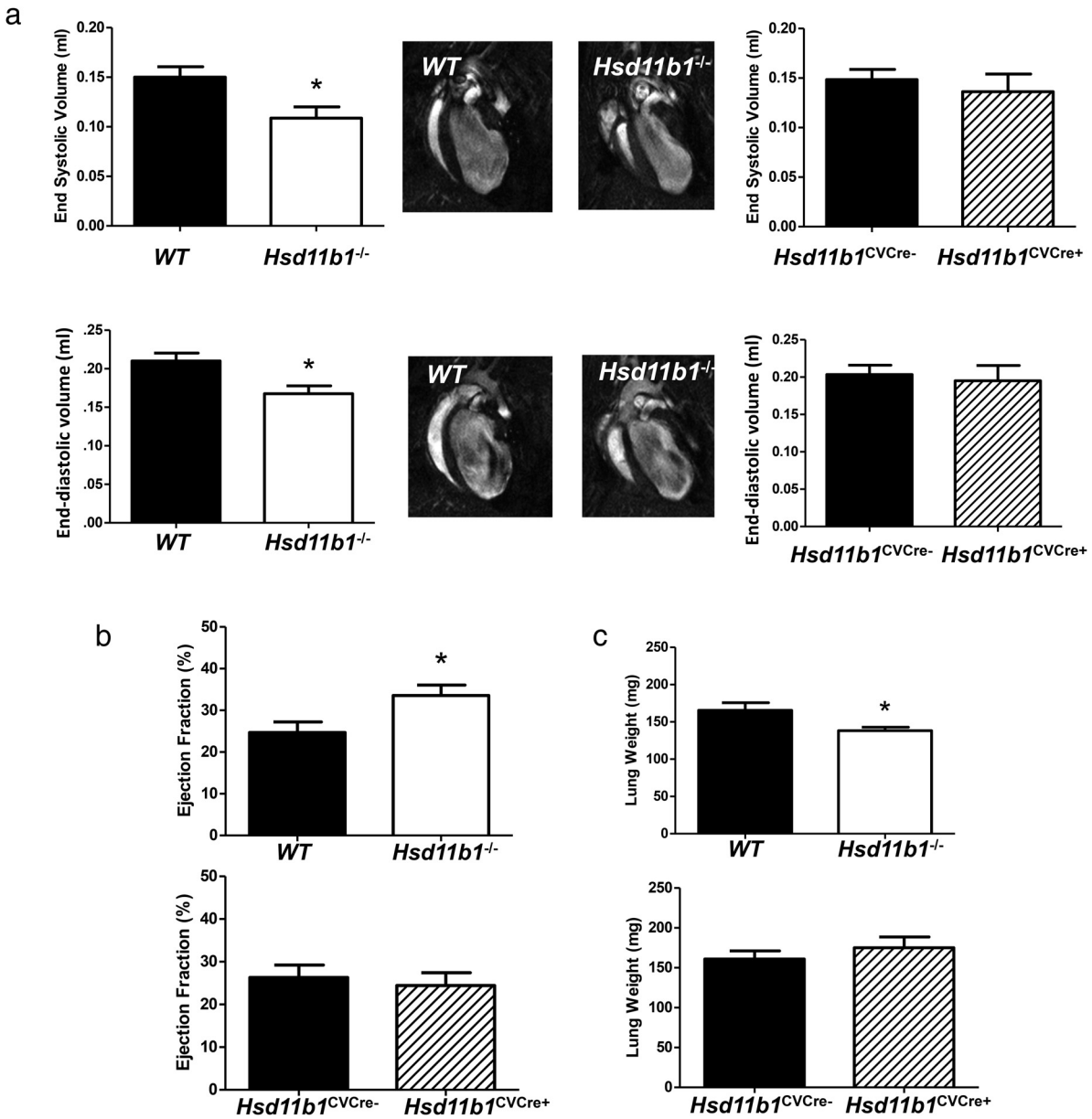

Figure 3. Global, but not cardiovascular, 11β-HSD1 deficiency reduces LV dilatation, loss of contractile function and pulmonary edema after MI. Structural (a) and functional (b) remodelling was compared by MRI in wild type (WT) and global 11β-HSD1 deficient mice (*hsd11b1*$^{-/-}$), and in mice with cardiomyocyte and vascular smooth muscle specific deletion (*hsd11b1*$^{CVCre+}$) and respective floxed control (*hsd11b1*$^{CVCre-}$) at 8 weeks after induction of MI by coronary artery ligation. The middle panels show 4 chamber views collected by cine-MRI at end-systole (top) and end-diastole (bottom). Lungs were collected from mice after imaging and weighed to detect pulmonary edema (c). Paired groups were compared by Student's *t* test * $P < .05$, ** $P < .01$, *** $P < .005$; n = 6–8/group.

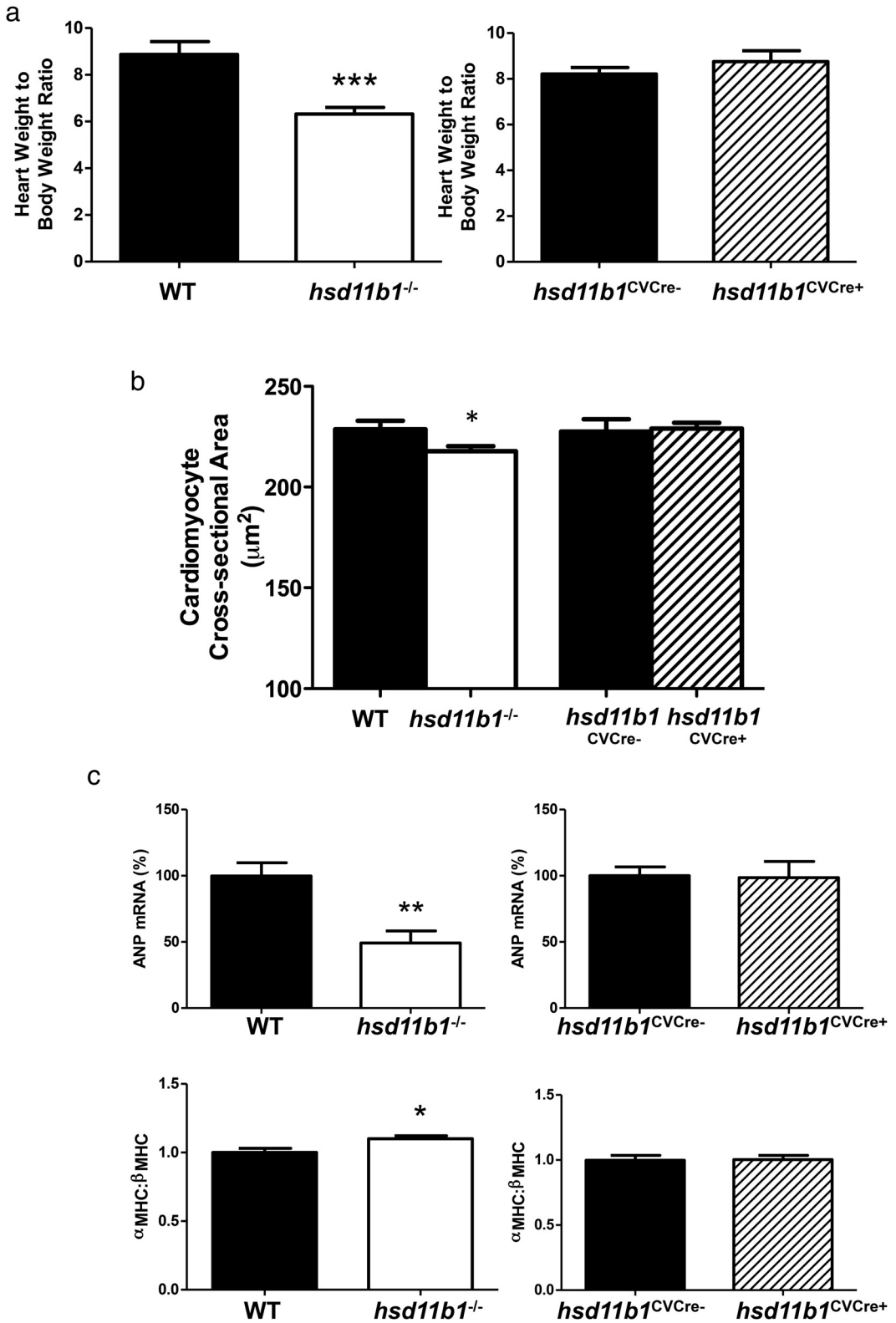

Figure 4. Hypertrophic remodeling and expression of fetal genes are inhibited in mice with global, but not cardiovascular, 11β HSD1 deficiency. Heart:body weight ratio (a) and cardiomyocyte cross-sectional area (b) were compared in mice global 11β-HSD1 deficient mice (*Hsd11b1*$^{-/-}$) and wild-type (WT) controls, and in mice with cardiomyocyte and vascular smooth muscle specific deletion (*Hsd11b1*$^{CVCre+}$) compared to respective floxed control (*Hsd11b1*$^{CVCre-}$) at 8 weeks after induction of MI by coronary artery ligation. (c) Expression of fetal genes atrial natriuretic peptide (ANP (*Nppa*)), upper panel) and α myosin heavy chain (αMHC (*Myh6*), expressed relative to βMHC (*Myh7*), lower panel) was determined by real-time PCR. * $P < .05$, ** $P < .01$, *** $P < .005$ vs matched control; n = 6–8/group.

endothelium, of murine vasculature (17), where it regulates inflammation and neointimal proliferation (40, 41). It has been suggested that 11β-HSD1 in the vessel wall may contribute to regulation of angiogenesis (10). However, in the present study targeted deletion of 11β-HSD1 in vascular smooth muscle failed to recapitulate enhancement of peri-infarct angiogenesis following MI. Enhancement of angiogenesis was previously linked to promotion of alternative macrophage activation during early infarct healing in globally *Hsd11b1* deficient mice (8), this was also absent in mice with targeted deletion of *Hsd11b1 in* cardiomyocytes and vascular smooth muscle. Again, other cells present in the heart, including fibroblasts and myeloid cells, express 11β-HSD1 and can release molecules that regulate inflammation and angiogenesis (36–38), and these sites may be important for the effects of global 11β-HSD1 deficiency on infarct healing post-MI. Alternative macrophage activation can also promote fibrosis (42), potentially having a detrimental influence on cardiac function in the longer term. However, there was no evidence in the present study for an influence of 11β-HSD1 deficiency on the expression of a range of fibrosis associated genes in the failing LV.

The discussions above are focused around the principal that the primary function of 11β-HSD1 is to modulate intracellular availability of active glucocorticoid metabolites. Evidence is provided for appropriate reduction of gene expression and protein content in mice with targeted deletion of *Hsdl11b1,* but a limitation of the study is the lack of direct evidence for reduction of active glucocorticoid regeneration through 11β-HSD1 activity in the targeted cells. While it is not therefore possible to state conclusively that reduced availability of locally generated glucocorticoids is key for the study outcomes, this limitation does not detract from the conclusion that 11β-HSD1 is a valid therapeutic target in the heart following MI.

A number of pharmacological inhibitors of 11β-HSD1 have been developed for the treatment of atherosclerotic

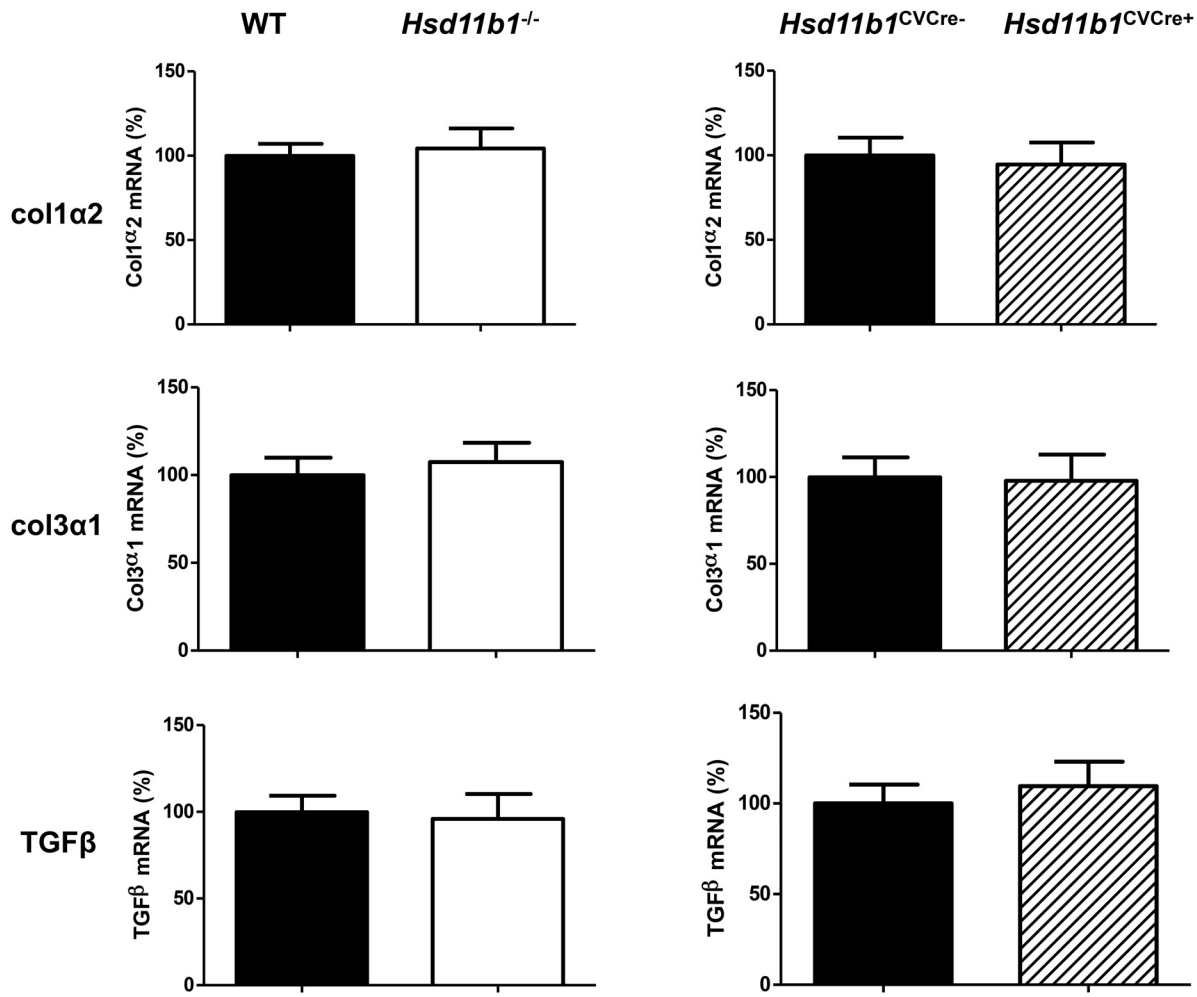

Figure 5. Fibrotic gene expression post-MI is not influenced by 11β-HSD1 Myocardial *Col1a2* (upper panel), *Col3a1* (middle panel) and *Tgfb1* (lower panel) expression determined by qRT-PCR in hearts from wild type mice (WT), mice with global depletion of 11β-HSD1 (*Hsd11b1*$^{-/-}$), mice with deletion in cardiac and vascular smooth muscle cells (*Hsd11b1*$^{CVCre+}$) and floxed Cre –ve controls (*Hsd11b1*$^{CVCre-}$); n = 6–8/group).

Table 1.

Peptide/protein target	Antigen sequence (if known)	Name of Antibody	Manufacturer, catalog #, and/or name of individual providing the antibody	Species raised in; monoclonal or polyclonal	Dilution used
Mac-2 (Galectin-3)		Anti-mouse/human Mac-2	Cedarlane, CL8942AP	Rat, monoclonal	1 in 6000
Ym-1 (ECF-L)		Ym1 antibody	Stem Cell Technologies, 01 404	Rabbit, polyclonal	1 in 500
CD 31 (Pecam)		Anti-CD-31 antibody	Abcam, ab28364	Rabbit, polyclonal	1 in 50
Isolectin B4		Isolectin GS-IB4 from griffonia simplifolica	Thermo Fisher, I21413	rabbit	1 in 100
wheat germ agglutinin		Rhodamine labelled wheat germ agglutinin	Vector Laboratoroes RL-1022	goat	1 in 75
β-actin		β-actin antibody	Cell Signalling Technology, 4967S	Rabbit, polyclonal	1 in 1000
11β-HSD1		11β-HSD1	Prof Karen Chapman	sheep	1 in 1000

and metabolic disease (15). We have found that 11β-HSD1 inhibitor can promote early angiogenesis and prevent infarct expansion when given immediately after MI (16), the present data suggests that pharmacological 11β-HSD1 inhibition also has the potential to reduce progression to heart failure. The use of mineralocorticoid receptor

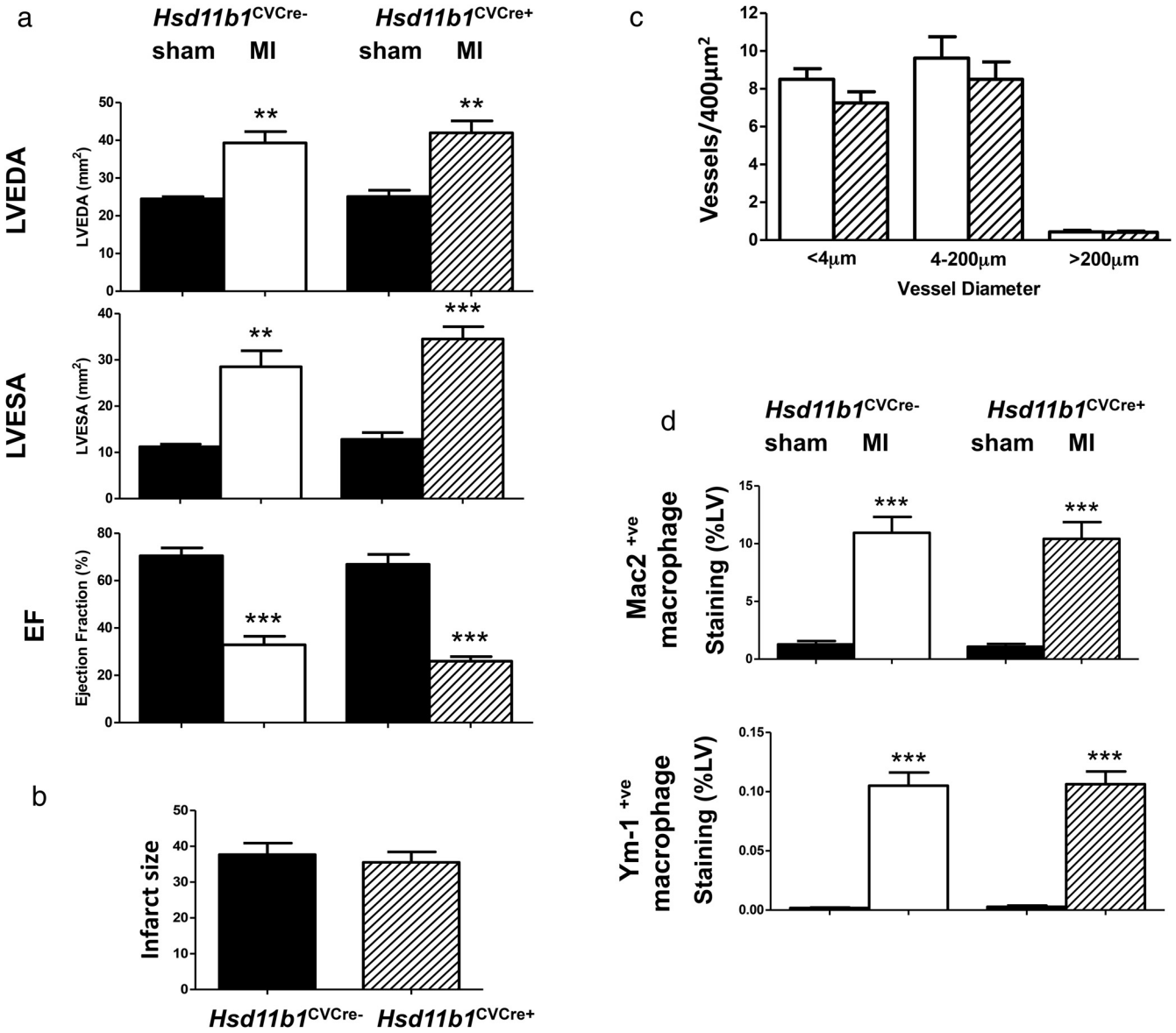

Figure 6. Cardiovascular selective deletion of 11βHSD1 does not modify early infarct healing Structural and functional remodelling (a), infarct size (b), peri-infarct angiogenesis (c), macrophage density and polarization (e), were all comparable in *Hsd11b1*$^{CVCre+ve}$ and control floxed mice (*Hsd11b1*$^{CVCre+ve}$) mice during infarct healing 7 days after induction of MI. Left ventricular end diastolic area (LVEDA), LV end systolic area (LVESA), fractional shortening (FS) and EF (EF) were assessed by high resolution ultrasound in mice 7 days after induction of MI by coronary artery ligation, or sham operation (sham). Macrophages were identified by immunoreactivity for the secreted protein Mac-2 (d, upper panel) and alternatively activated macrophages by expression of immunoreactive Ym-1 (d, lower panel). ** $P < .01$, *** $P < .005$. vs sham of same genotype, n = 8/group.

(MR) antagonists in patients with heart failure is now well established (43). Recent clinical and experimental studies have highlighted additional benefits of MR antagonists when given early after MI, that include promotion of angiogenesis and prevention of infarct expansion (44, 45). Studies in mice with cardiomyocyte-restricted inactivation of the MR gene suggest that the clinical benefits of MR blocking therapy in MI and heart failure are mediated largely via cardiomyocyte-dependent mechanisms (46). As the present data show that the effects of *Hsd11b1* gene targeting are cardiomyocyte independent, 11β-HSD1 inhibitors may offer additional benefits in patients already receiving MR antagonist therapy or an alternative in patients for whom hyperkalemia precludes the use of MR antagonists (47).

Acknowledgments

The authors acknowledge the technical assistance of Ross Lennen (MRI) and are grateful to Ms Tak-Yun Man for the generation and breeding of *Hsd11b1*^{CVCre} mice.

Address all correspondence and requests for reprints to: *Dr Gillian A Gray, BHF/University Centre for Cardiovascular Science, The University of Edinburgh, Queens Medical Research Institute, 47 Little France Crescent, Edinburgh, EH14 6TJ, Scotland, UK, *tel*: (44) 131 242 9213, *email:* gillian.gray@ed.ac.uk.

Disclosure Summary: CIW, MAJ, KM, AT, RVR, CMM, KJM, KEC & GAG have nothing to declare. BRW and JRS are inventors on relevant patents owned by the University of Edinburgh and licensed to Actinogen Medical, for whom BRW acts as a Consultant.

This work was supported by the Wellcome Trust (WT091720MA and WT083184). CIW was the recipient of a British Heart Foundation 4 year PhD studentship (FS/09/053). The Centre for Cardiovascular Science is supported by a British Heart Foundation Centre of Research Excellence Award.

References

1. **Danchin N.** Winning the battle against ST-segment-elevation myocardial infarction: continued progress, but still a long way to go. *Eur Heart J*. 2010;31:2580–2582.
2. **Bolognese L, Neskovic AN, Parodi G, Cerisano G, Buonamici P, Santoro GM, Antoniucci D.** Left ventricular remodeling after primary coronary angioplasty: patterns of left ventricular dilation and long-term prognostic implications. *Circulation*. 2002;106:2351–2357.
3. **Ibanez B, Heusch G, Ovize M, Van de Werf F.** Evolving Therapies for Myocardial Ischemia/Reperfusion Injury. *J Am Coll Cardiol* 2015;65:1454–1471.
4. **Sluijter JP, Condorelli G, Davidson SM, Engel FB, Ferdinandy P, Hausenloy DJ, Lecour S, Madonna R, Ovize M, Ruiz-Meana M, Schulz R, Van Laake LW.** Novel therapeutic strategies for cardioprotection. *Pharmacol Ther*. 2014;144:60–70.
5. **Cochain C, Channon KM, Silvestre JS.** Angiogenesis in the infarcted myocardium. *Antioxid Redox Signal*. 2013;18:1100–1113.
6. **Emanueli C, Madeddu P.** Therapeutic angiogenesis: translating experimental concepts to medically relevant goals. *Vascul Pharmacol*. 2006;45:334–339.
7. **Loke P, Nair MG, Parkinson J, Guiliano D, Blaxter M, Allen JE.** IL-4 dependent alternatively-activated macrophages have a distinctive in vivo gene expression phenotype. *BMC Immunology*. 2002;3:7.
8. **McSweeney SJ, Hadoke PW, Kozak AM, Small GR, Khaled H, Walker BR, Gray GA.** Improved heart function follows enhanced inflammatory cell recruitment and angiogenesis in 11betaHSD1-deficient mice post-MI. *Cardiovasc Res*. 2010;88:159–167.
9. **Meloni M, Marchetti M, Garner K, Littlejohns B, Sala-Newby G, Xenophontos N, Floris I, Suleiman MS, Madeddu P, Caporali A, Emanueli C.** Local inhibition of microRNA-24 improves reparative angiogenesis and left ventricle remodeling and function in mice with myocardial infarction. *Mol Ther*. 2013;21:1390–1402.
10. **Small GR, Hadoke PW, Sharif I, Dover AR, Armour D, Kenyon CJ, Gray GA, Walker BR.** Preventing local regeneration of glucocorticoids by 11beta-hydroxysteroid dehydrogenase type 1 enhances angiogenesis. *Proc Natl Acad Sci U S. A*. 2005;102:12165–12170.
11. **LeGal YM, Morrissey LL.** Methylprednisolone interventions in myocardial infarction: a controversial subject. *Can J Cardiol*. 1990;6:405–410.
12. **Libby P, Maroko PR, Bloor CM, Sobel BE, Braunwald E.** Reduction of experimental myocardial infarct size by corticosteroid administration. *J Clin Invest*. 1973;52:599–607.
13. **Mihailidou AS, Loan Le TY, Mardini M, Funder JW.** Glucocorticoids activate cardiac mineralocorticoid receptors during experimental myocardial infarction. *Hypertension*. 2009;54:1306–1312.
14. **Chapman K, Holmes M, Seckl J.** 11beta-hydroxysteroid dehydrogenases: intracellular gate-keepers of tissue glucocorticoid action. *Physiol Rev*. 2013;93:1139–1206.
15. **Anderson A, Walker BR.** 11beta-HSD1 inhibitors for the treatment of type 2 diabetes and cardiovascular disease. *Drugs* 2013;73:1385–1393.
16. **McGregor K, Webster S, Mylonas K, White CI, Walker BR, Gray G.** Immediate pharmacological inhibition of local glucocorticoid generation increases angiogenesis and improves cardiac function after myocardial infarction. *Heart* 2014;100 (Supp 3):A118.
17. **Christy C, Hadoke PW, Paterson JM, Mullins JJ, Seckl JR, Walker BR.** 11beta-hydroxysteroid dehydrogenase type 2 in mouse aorta: localization and influence on response to glucocorticoids. Hypertension 2003;42:580–587.
18. **Dover AR, Hadoke PW, Macdonald LJ, Miller E, Newby DE, Walker BR.** Intravascular glucocorticoid metabolism during inflammation and injury in mice. *Endocrinology*. 2007;148:166–172.
19. **Gordon O, He Z, Gilon D, Gruener S, Pietranico-Cole S, Oppenheim A, Keshet E.** A transgenic platform for testing drugs intended for reversal of cardiac remodeling identifies a novel 11betaHSD1 inhibitor rescuing hypertrophy independently of re-vascularization. *PLoS One* 2014; 9:e92869.
20. **Kipari T, Hadoke PW, Iqbal J, Man TY, Miller E, Coutinho AE, Zhang Z, Sullivan KM, Mitic T, Livingstone DE, Schrecker C, Samuel K, White CI, Bouhlel MA, Chinetti-Gbaguidi G, Staels B, Andrew R, Walker BR, Savill JS, Chapman KE, Seckl JR.** 11beta-hydroxysteroid dehydrogenase type 1 deficiency in bone marrow-derived cells reduces atherosclerosis. *FASEB J*. 2013;27:1519–1531.
21. **Lepore JJ, Cheng L, Min Lu M, Mericko PA, Morrisey EE, Parmacek MS.** High-efficiency somatic mutagenesis in smooth muscle cells and cardiac myocytes in SM22alpha-Cre transgenic mice. *Genesis*. 2005;41:179–184.
22. **Wang Y, Cao Y, Yamada S, Thirunavukkarasu M, Nin V, Joshi M, Rishi MT, Bhattacharya S, Camacho-Pereira J, Sharma AK, Shameer K, Kocher JP, Sanchez JA, Wang E, Hoeppner LH, Dutta SK, Leof EB, Shah V, Claffey KP, Chini EN, Simons M, Terzic A,**

Maulik N, Mukhopadhyay D. Cardiomyopathy and Worsened Ischemic Heart Failure in SM22-alpha Cre-Mediated Neuropilin-1 Null Mice: Dysregulation of PGC1alpha and Mitochondrial Homeostasis. *Arterioscler Thromb Vasc Biol*. 2015;35:1401–1412.

23. **Gray GA, Patrizio M, Sherry L, Miller AA, Malaki M, Wallace AF, Leiper JM, Vallance P.** Immunolocalisation and activity of DDAH I and II in the heart and modification post-myocardial infarction. *Acta Histochem*. 2010;112:413–423.
24. **O'Brien PJ, Smith DE, Knechtel TJ, Marchak MA, Pruimboom-Brees I, Brees DJ, Spratt DP, Archer FJ, Butler P, Potter AN, Provost JP, Richard J, Snyder PA, Reagan WJ.** Cardiac troponin I is a sensitive, specific biomarker of cardiac injury in laboratory animals. *Lab Anim*. 2006;40:153–171.
25. **Gray GA, White CI, Thomson A, Kozak A, Moran C, Jansen MA.** Imaging the healing murine myocardial infarct in vivo: ultrasound, magnetic resonance imaging and fluorescence molecular tomography. *Exp Physiol*. 2013;98:606–613.
26. **De Sousa Peixoto RA, Turban S, Battle JH, Chapman KE, Seckl JR, Morton NM.** Preadipocyte 11beta-hydroxysteroid dehydrogenase type 1 is a keto-reductase and contributes to diet-induced visceral obesity in vivo. *Endocrinology*. 2008;149:1861–1868.
27. **Schultz Jel J, Witt SA, Glascock BJ, Nieman ML, Reiser PJ, Nix SL, Kimball TR, Doetschman T.** TGF-beta1 mediates the hypertrophic cardiomyocyte growth induced by angiotensin II. *J Clin Invest*. 2002;109:787–796.
28. **Protti A, Dong X, Sirker A, Botnar R, Shah AM MR.** I-based prediction of adverse cardiac remodeling after murine myocardial infarction. *Am J Physiol Heart Circ Physiol*. 2012;303:H309–314.
29. **Gaudron P, Kugler I, Hu K, Bauer W, Eilles C, Ertl G.** Time course of cardiac structural, functional and electrical changes in asymptomatic patients after myocardial infarction: their inter-relation and prognostic impact. *J Am Coll Cardiol*. 2001;38:33–40.
30. **Panagopoulou V, Deftereos S, Kossyvakis C, Raisakis K, Giannopoulos G, Bouras G, Pyrgakis V, Cleman.** MW NTproBNP: an important biomarker in cardiac diseases. *Curr Top Med Chem*. 2013; 13:82–94.
31. **Krenz M, Sanbe A, Bouyer-Dalloz F, Gulick J, Klevitsky R, Hewett TE, Osinska HE, Lorenz JN, Brosseau C, Federico A, Alpert NR, Warshaw DM, Perryman MB, Helmke SM, Robbins J.** Analysis of myosin heavy chain functionality in the heart. *J Biol Chem*. 2003; 278:17466–17474.
32. **Rahman TJ, Mayosi BM, Hall D, Avery PJ, Stewart PM, Connell JM, Watkins H, Keavney B.** Common variation at the 11-beta hydroxysteroid dehydrogenase type 1 gene is associated with left ventricular mass. *Circ Cardiovasc Genet*. 2011;4:156–162.
33. **Furtado MB, Costa MW, Pranoto EA, Salimova E, Pinto AR, Lam NT, Park A, Snider P, Chandran A, Harvey RP, Boyd R, Conway SJ, Pearson J, Kaye DM, Rosenthal NA.** Cardiogenic genes expressed in cardiac fibroblasts contribute to heart development and repair. *Circ Res*. 2014;114:1422–1434.
34. **Turner NA.** Effects of interleukin-1 on cardiac fibroblast function: relevance to post-myocardial infarction remodelling. *Vascul Pharmacol*. 2013;60:1–7.
35. **Fujiu K, Nagai R.** Fibroblast-mediated pathways in cardiac hypertrophy. *J Mol Cell Cardiol*. 2014;70:64–73.
36. **Hardy R, Juarez M, Naylor A, Tu J, Rabbitt EH, Filer A, Stewart PM, Buckley CD, Raza K, Cooper MS.** Synovial DKK1 expression is regulated by local glucocorticoid metabolism in inflammatory arthritis. *Arthritis Res Therap*. 2012;14:R226.
37. **Hardy RS, Filer A, Cooper MS, Parsonage G, Raza K, Hardie DL, Rabbitt EH, Stewart PM, Buckley CD, Hewison M.** Differential expression, function and response to inflammatory stimuli of 11beta-hydroxysteroid dehydrogenase type 1 in human fibroblasts: a mechanism for tissue-specific regulation of inflammation. *Arthritis ResTherap*. 2006; 8:R108.
38. **Chapman KE, Coutinho AE, Zhang Z, Kipari T, Savill JS, Seckl JR.** Changing glucocorticoid action: 11beta-hydroxysteroid dehydrogenase type 1 in acute and chronic inflammation. *J Steroid Biochem Mol Biol*. 2013;137:82–92.
39. **Singh MV, Chapleau MW, Harwani SC, Abboud FM.** The immune system and hypertension. *Immunol Res*. 2014;59:243–253.
40. **Hadoke PW, Kipari T, Seckl JR, Chapman KE.** Modulation of 11beta-hydroxysteroid dehydrogenase as a strategy to reduce vascular inflammation. *Curr Atheroscler Rep*. 2013;15:320.
41. **Iqbal J, Macdonald LJ, Low L, Seckl JR, Yau CW, Walker BR, Hadoke PW.** Contribution of endogenous glucocorticoids and their intravascular metabolism by 11beta-HSDs to postangioplasty neointimal proliferation in mice. *Endocrinology*. 2012;153:5896–5905.
42. **Mylonas KJ, Jenkins SJ, Castellan RF, Ruckerl D, McGregor K, Phythian-Adams AT, Hewitson JP, Campbell SM, MacDonald AS, Allen JE, Gray GA.** The adult murine heart has a sparse, phagocytically active macrophage population that expands through monocyte recruitment and adopts an 'M2' phenotype in response to Th2 immunologic challenge. *Immunobiology*. 2015;220:924–933.
43. **Zannad F, Gattis Stough W, Rossignol P, Bauersachs J, McMurray JJ, Swedberg K, Struthers AD, Voors AA, Ruilope LM, Bakris GL, O'Connor CM, Gheorghiade M, Mentz RJ, Cohen-Solal A, Maggioni AP, Beygui F, Filippatos GS, Massy ZA, Pathak A, Pina IL, Sabbah HN, Sica DA, Tavazzi L, Pitt B.** Mineralocorticoid receptor antagonists for heart failure with reduced ejection fraction: integrating evidence into clinical practice. *Eur Heart J*. 2012;33:2782–2795.
44. **Montalescot G, Pitt B, Lopez de Sa E, Hamm CW, Flather M, Verheugt F, Shi H, Turgonyi E, Orri M, Vincent J, Zannad F.** Early eplerenone treatment in patients with acute ST-elevation myocardial infarction without heart failure: the Randomized Double-Blind REMINDER Study. *Eur Heart J*. 2014;35:2295–2302.
45. **Fraccarollo D, Galuppo P, Schraut S, Kneitz S, van Rooijen N, Ertl G, Bauersachs J.** Immediate mineralocorticoid receptor blockade improves myocardial infarct healing by modulation of the inflammatory response. *Hypertension*. 2008;51:905–914.
46. **Fraccarollo D, Berger S, Galuppo P, Kneitz S, Hein L, Schutz G, Frantz S, Ertl G, Bauersachs J.** Deletion of cardiomyocyte mineralocorticoid receptor ameliorates adverse remodeling after myocardial infarction. *Circulation*. 2011;123:400–408.
47. **Rossignol P, Dobre D, McMurray JJ, Swedberg K, Krum H, van Veldhuisen DJ, Shi H, Messig M, Vincent J, Girerd N, Bakris G, Pitt B, Zannad F.** Incidence, determinants, and prognostic significance of hyperkalemia and worsening renal function in patients with heart failure receiving the mineralocorticoid receptor antagonist eplerenone or placebo in addition to optimal medical therapy: results from the Eplerenone in Mild Patients Hospitalization and Survival Study in Heart Failure (EMPHASIS-HF). *Circ Heart Fail*. 2013;7: 51–58.